www.czasopisma.pan.pl PAN POLSKA AKADEMIA NAUK www.journals.pan.pl

PAN ARCHIVES OF ACOUSTICS
Vol. 41, No. 1, pp. 87–97 (2016)

DOI: 10.1515/aoa-2016-0009

The Effect of the Cavity Damping on Vehicular Evaluation using the Finite Element Method

Tiago S. FERREIRA(1), Pedro A. MAGALHÃES(1),
Frederico L. MOURA(2), Timoteo S. FERREIRA(2)

(1) *Department of Mechanical Engineering, Pontifical University Catholic*
Av. Dom José Gaspar, 500, Belo Horizonte, Brazil;
e-mail: tiago.simao@ifmg.edu.br, paamj@oi.com.br

(2) *Department of Mechanical Engineering, Federal University of Minas Gerais*
Av. Antônio Carlos, 6627 – Pampulha, Belo Horizonte, Brazil;
e-mail: {frediluiz, timoteo_ferreira}@yahoo.com.br

(*received November 7, 2014; accepted November 2, 2015*)

This work focuses on finding a numerical solution for vehicle acoustic studies and improving the usefulness of the numerical experimental parameters for the development stage of a new automotive project. Specifically, this research addresses the importance of modal cavity damping for vehicle exerts during numerical studies. It then seeks to suggest standardized parameter values of modal cavity damping in vehicular acoustic studies.

The standardized value of modal cavity damping is of great importance for the study of vehicular acoustics in the automotive industry because it would allow the industry to begin studies of the acoustic performance of a new vehicle early in the conception phase with a reliable estimation that would be close to the final value measured in the design phase. It is common for the automotive industry to achieve good levels of numerical-experimental correlation in acoustic studies after the prototyping phase because this phase can be studied with feedback from the simulation and experimental modal parameters.

Thus, this research suggests values for modal cavity damping, which are divided into two parts due to their behaviour: $\xi(x) = -0.0126(x - 100) + 6.15$ as a variable function to analyse up to 100 Hz and 6.15% of modal cavity damping constant for studies between 30 Hz and 100 Hz.

The sequence of this study shows how we arrived at these values.

Keywords: finite element methods; acoustic control; trimmed body; numerical experimental correlation; modal damping.

1. Introduction

This study has been motivated by the conflict during the final stages of the development of a vehicle, as well as by the comparison between the results generated by the simulation team with those acquired from the experimental team.

For an appropriate correlation, it is always necessary to acquire modal cavity damping data originated from prototypes and subsequently assign them to the numerical model. In this manner, the phase of refinement of the numerical results requires a prototype, and this slows the progress of work and research.

With respect to simulation methods used today, the finite element method (FEM), as described by Braess, Seiffert (2005), the situation is quite different as it enables conducting studies with quickness and agility. Ever-increasing demands for greater comfort have elevated the dynamic design criteria as the primary elements of modern body engineering.

Damping and sound-insulation measures are strictly applied to automotive body panels to prevent noise in the vehicle cabin (Lim, 2000; Kurosawa, Yamaguchi, 2013). Automotive body panels, which are made of steel sheets press-molded into a required form, are laminated with damping materials to reduce the vibration level. Furthermore, porous media, resin sheets (surface), and carpet are laminated onto the damping materials (Davy *et al.*, 2014; Pockszevnicki *et al.*, 2011; Zhang *et al.*, 2005).

For this study 2 (two) different categories of vehicles were investigated: a pick-up truck and a popular compact vehicle. Hence, the study is expected to determine a range of values that cover the cavity damping behaviour by analysing these vehicles in the Trimmed-Body configuration (Hörnlund, Papazoglu, 2005).

Acoustic FEM analysis of the system was performed using standard MSC Nastran 2010 software. Following the FEM analysis, a modal analysis of the entire vehicle and cavity was performed; the data were treated as described by Moura *et al.* (2012), in CRF VEIPROD 5.0® software for the evaluation of the SPL (Sound Pressure level).

With respect to the experimental data campaign, the bodyshell (TBIW – trimmed body) testing was performed in a laboratory at NVH in a semi-anechoic room, exploiting LMS Test Lab 11B (2013).

Finally, this research work seeks to accomplish the following:

A) Determine the influence of the observed modal cavity damping variation in the physical testing on the simulation models, seeking to better identify the existence of the resonance modes between the cavity and body-shell.

B) Propose a medium modal cavity damping (Cavity Damping Design) that can be used even in the early stages of vehicle development and provide results similar to those generated using the actual variable damping.

Figure 1 shows a schematic flowchart of the ideas presented previously.

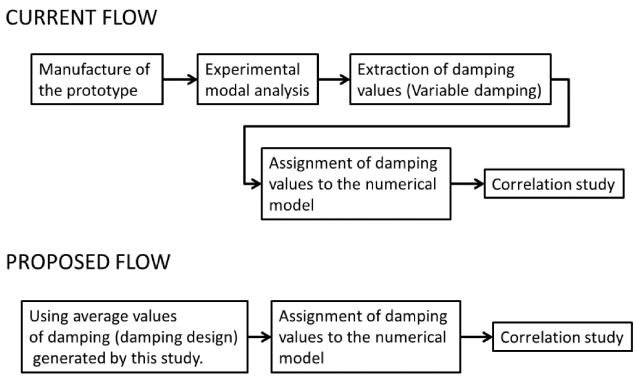

Fig. 1. Flowchart of job steps (current and proposed).

The step "correlation study" corresponds to the moment where the experimental data will be compared with those obtained numerically.

2. Experimental methodology

As part of the validation process of the numerical experiment, the first step adopted in this study was to perform experimental modal analysis of the cavity, in which one expects a correlation regarding the global modes, and to determine how the damping behaviour of these cavities would vary in frequency when comparing various types of vehicles (Cameron *et al.*, 2010; Kumar *et al.*, 2013).

Consequently, all vehicles (two from different categories) underwent the same instrumentation as shown in Figs. 2 and 3. The experimental results were obtained by processing the data using LMS Test Lab 11B software. Table 1 shows the list of equipment used for the experimental measurements.

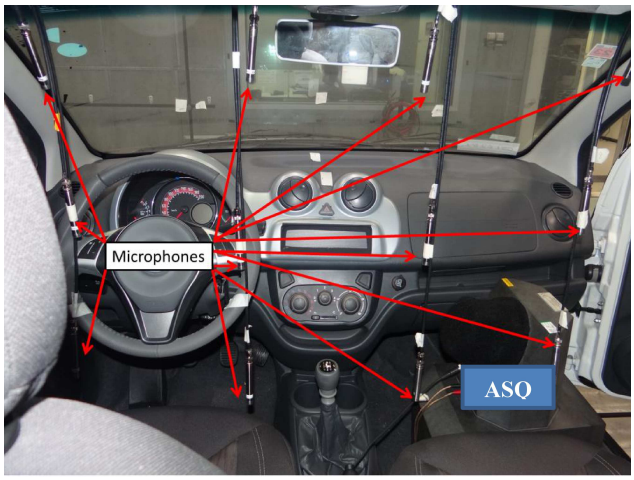

Fig. 2. Instrumentation for modal cavity analysis.

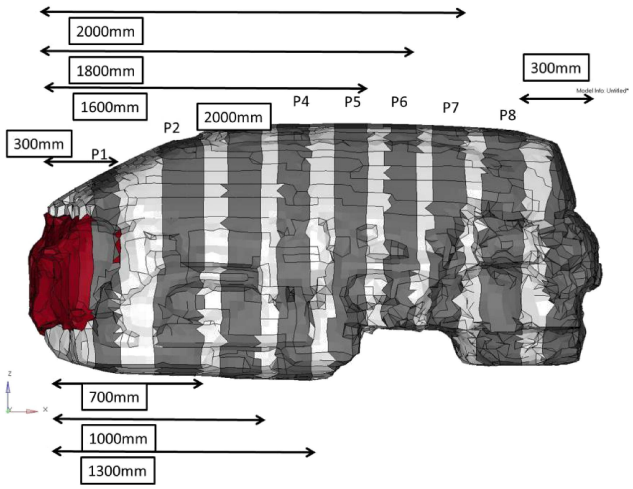

Fig. 3. Measurement planes – modal cavity.

Table 1. List of equipment.

Equipment	Sensitivity/Details
ASQ (Acoustic Source quantification)	41.15 mV/m^3/s^2
Microphone	50 mV/Pa
LMS Test Lab	Scadas Mobile – Modulo spectral Testing

The vehicle (TBIW) is placed in an acoustic chamber (isolated) with the glass windows closed; a random noise source is placed inside the front and rear of

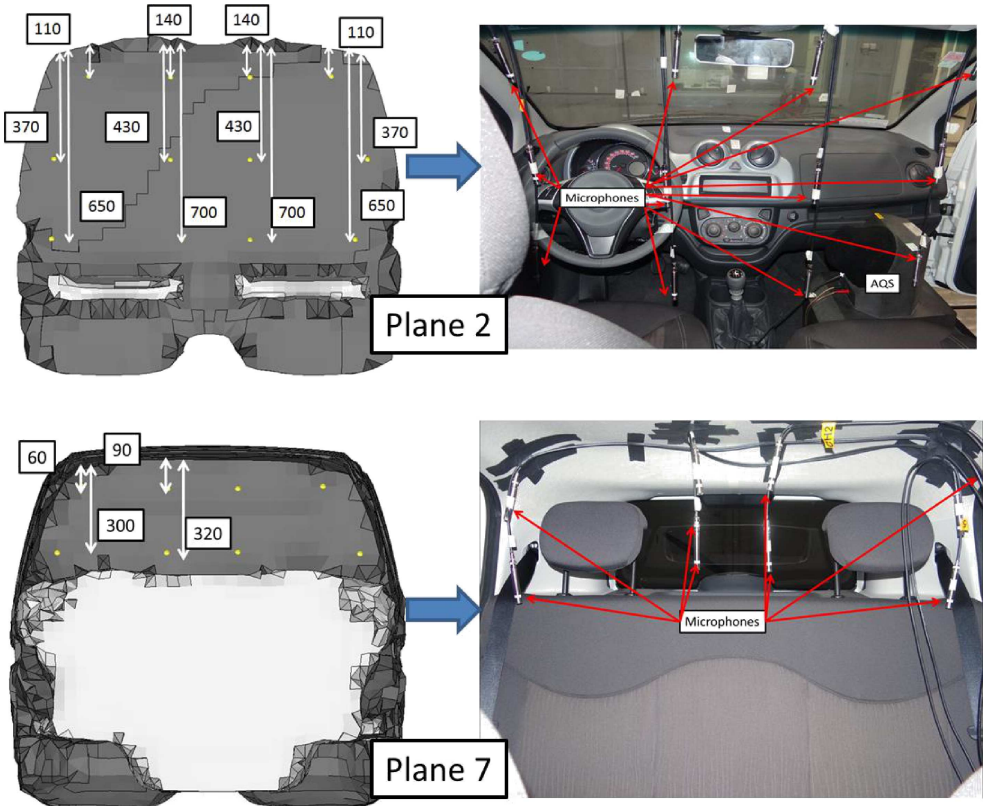

Fig. 4. Measurement plans definition.

the vehicle for reciprocal testing, and the vehicle has a cavity internally divided into planes defined by microphone chains. The excitation measured by the microphones (SPL – Sound Pressure Level) defines the modal behaviour of the cavity of the vehicle.

Placement of microphones is presented in Fig. 3 and Fig. 4.

On the left-hand side of Fig. 4, the numbers mean the distance in millimeters from the roof to the positioning of the microphones.

Planes P2 and P7 were chosen to represent the performance of the instrumentation process of the vehicle. This example is shown in Fig. 4.

For the initial assessment of the vehicle cavity modal behaviour in the early stages of its development, the frequency response functions, known as "SPL", are analysed at the various points of the microphone positions in the trimmed-body configuration. The FRF "SPL" provides the ratio of (P/F), where P is the pressure [dB] and F is the force [N] of an excitation point on the structure. The vehicle model is evaluated with the response measured at the points indicated in planes shown in Fig. 3.

In Fig. 5, an example of the results of the experimental cavity modal analysis is shown; all vehicles were subjected to the same test.

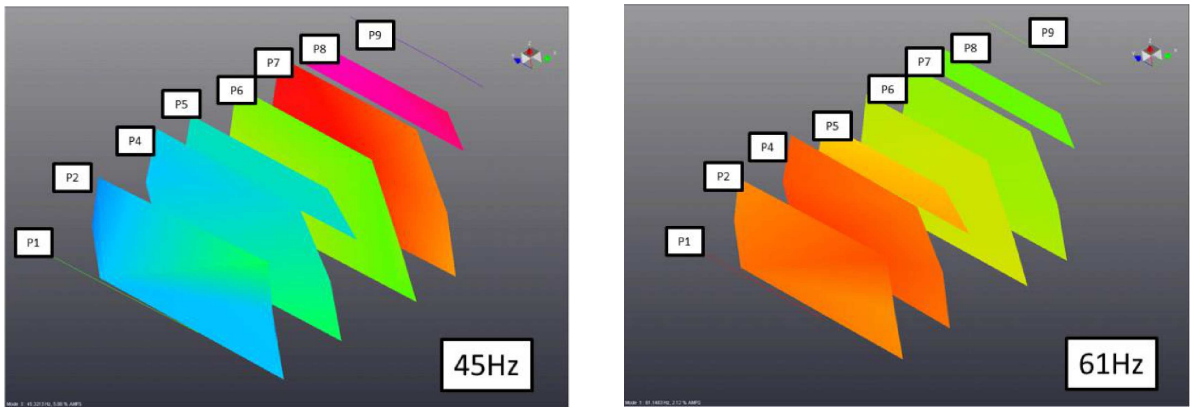

Fig. 5. Experimental cavity modal analysis of the studied vehicles.

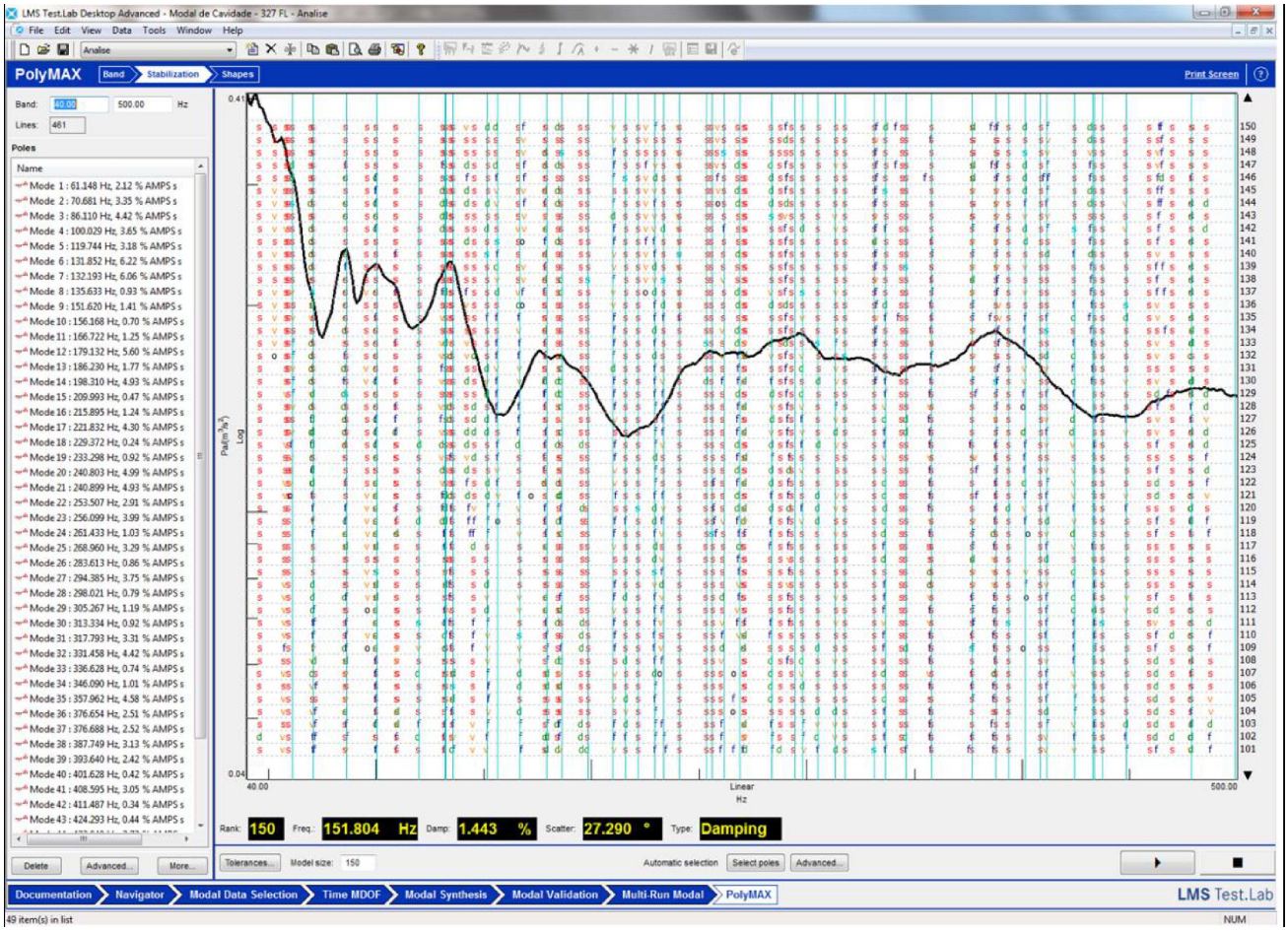

Fig. 6. Cavity modal analysis processed by the LMS-PolyMax method.

After plane-by-plane measurements were made, the results were compiled and processed by the LMS-PolyMax (Modulo spectral Testing) method. Figure 6 shows this processing; the left-hand side is presented in addition to the overall mode of the cavity, the main modal frequencies of the cavity, and its damping. The middle line of this measurement is highlighted at the centre of the figure.

PolyMAX is based on a (weighted) least-squares approach and uses multiple-input-multiple-output frequency response functions as primary data. This so-called "PolyMAX" or polyreference least-squares complex frequency-domain method can be implemented in a very similar way as the industry standard polyreference (time-domain) least-squares complex exponential method: in a first step a stabilization diagram is constructed containing frequency, damping, and participation information. Next, the mode shapes are found in a second least-squares step, based on the user selection of stable poles. One of the specific advantages of the technique lies in the very stable identification of the system poles and participation factors as a function of the specified system order, leading to easy-to-interpret stabilization diagrams (Peeters *et al.*, 2004).

Figure 7 presents the results of cavity modal analysis. When the measurements were complete, it was possible to extract the modal behaviour (Cavity Damping factor) of all vehicles (the two different categories of vehicles) and analyse the results to obtain the value of each modal damping (Hörnlund, Papazoglu, 2005, Rao, Singiresu, 2008) of the cavity along the frequency (actual variable damping). This response is presented in Fig. 7; the damping factor was extracted from a frequency (Hz) sweep.

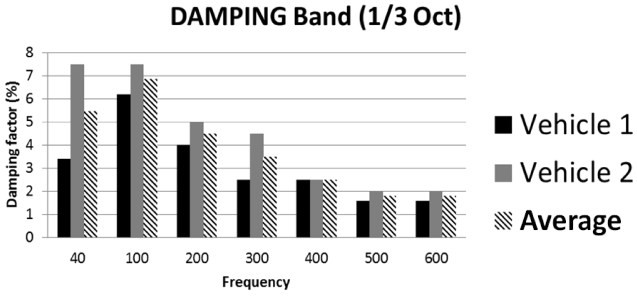

Fig. 7. Damping factor response in frequency for different vehicles.

The half-power method was used to find the damping value. Half-power bandwidth is defined as the ra-

tio of the frequency range between the two half power points to the natural frequency at this mode. Below is the manual equation for the half power calculation.

$$\xi = ([f_1 - f_2]/f_{\text{res}}), \tag{1}$$

where ξ is the damping factor and the f_1 and f_2 are the frequencies corresponding to an amplitude of $f_{\text{res}}/\sqrt{2}$. Thus, although the analysis presented in Fig. 7 covers the frequency range of 0–500 Hz, the results of the damping factor (%) appear only starting at the 1/3 octave band of 40 Hz where the first natural modes of the cavity begin.

Next, the modal test vehicles were characterised to determine the dynamic "SPL" type. This test is performed with microphones positioned at the height of the right ear of the driver that collected the data as acoustic pressure was generated.

Figures 8 and 9 illustrate the excitation points used by the team during the experimental tests. The impact generated by the impact hammer occurred directly adjacent to the accelerometer presented in this figure.

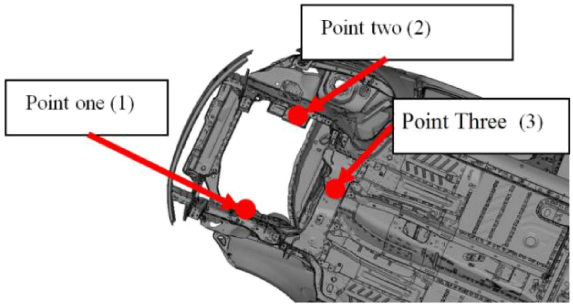

Fig. 8. Layout of the experimental test, bottom view (point 1, 2, and 3).

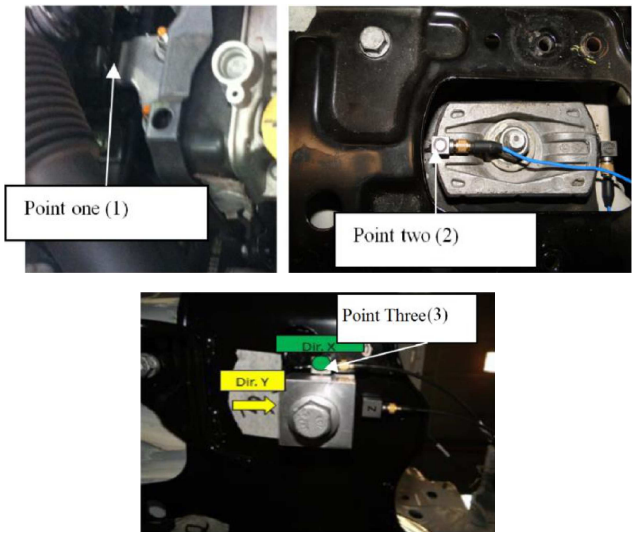

Fig. 9. Layout of the experimental test, engine mount (point 1, 2, and 3).

After defining the excitation points, the measured acoustic point detailed above is presented in Fig. 10 in a Standard Fiat (Performance Standard, 2004). The

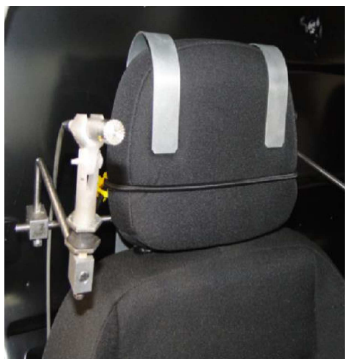

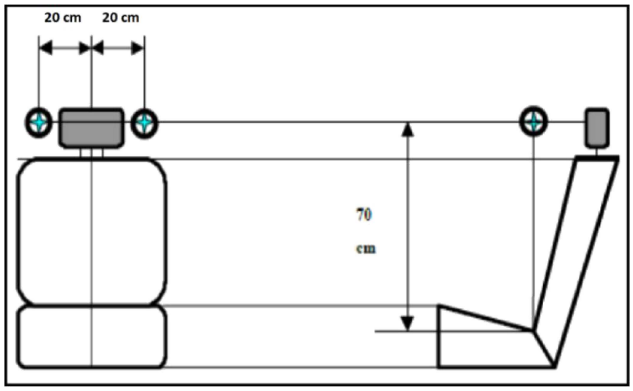

Fig. 10. Experimental configuration of the microphone position (the point of measurement).

figure presents the fixation point of the microphone at the height of the driver's right ear (left side of the figure) and details the microphone positioning (right side of the figure).

With respect to the experimental data campaign, full vehicle testing was performed in a laboratory at NVH in a semi-anechoic room, using LMS Test Lab 11B software. Table 2 shows the list of equipment used for the experimental measurements.

Table 2. List of equipment.

Equipment	Sensitivity/Details
Impact Hammer	2 mV/N
Microphone	50 mV/Pa
LMS Test Lab	Scadas Mobile – Modulo Impact Testing

The following results allow a comparison with numerical results; therefore, the frequency range used in this study is 0–500 Hz. The new frequency range was selected to concentrate on the influence of damping and avoid any influences caused by numerical errors in high frequency (Ferreira *et al.*, 2013).

The results of the "SPL" of the settings shown previously are displayed in Figs. 11 (Pickup) and 12 (popular compact vehicle). All of the results bellow were collected at the point illustrated in Fig. 9 and are on a logarithmic scale.

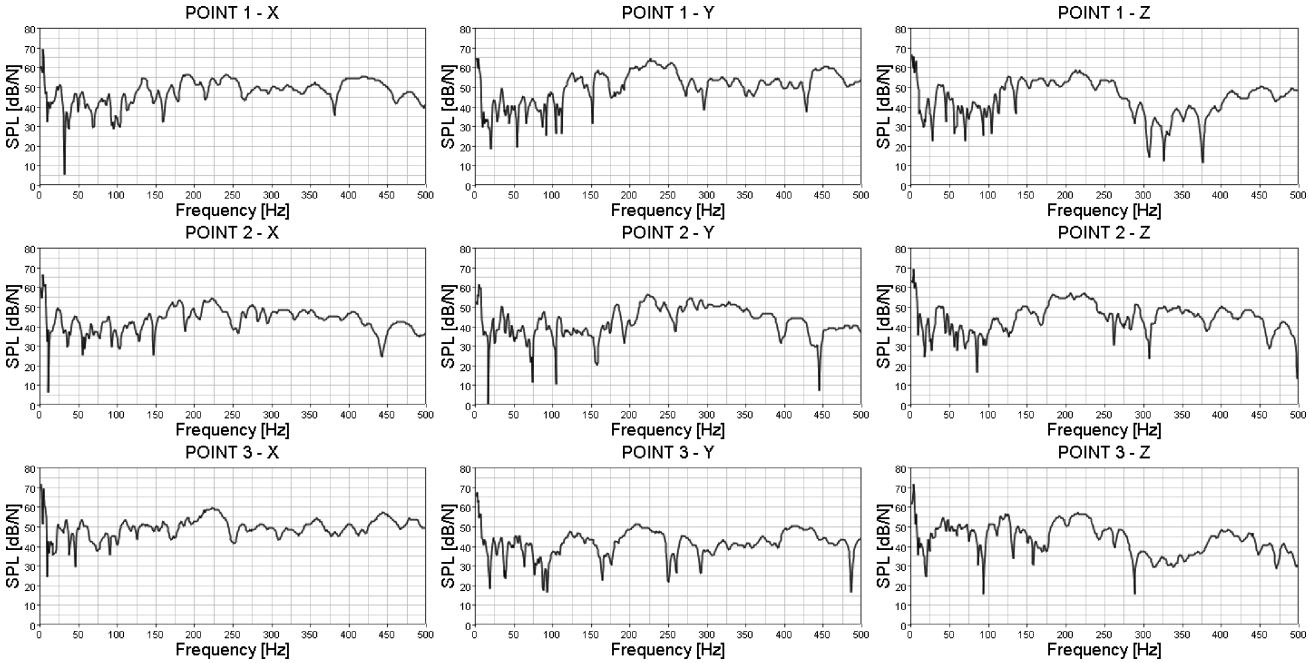

Fig. 11. Pickup model. SPL experimental response of the attachment point of the engine (the ordinate grid step is LOG scale).

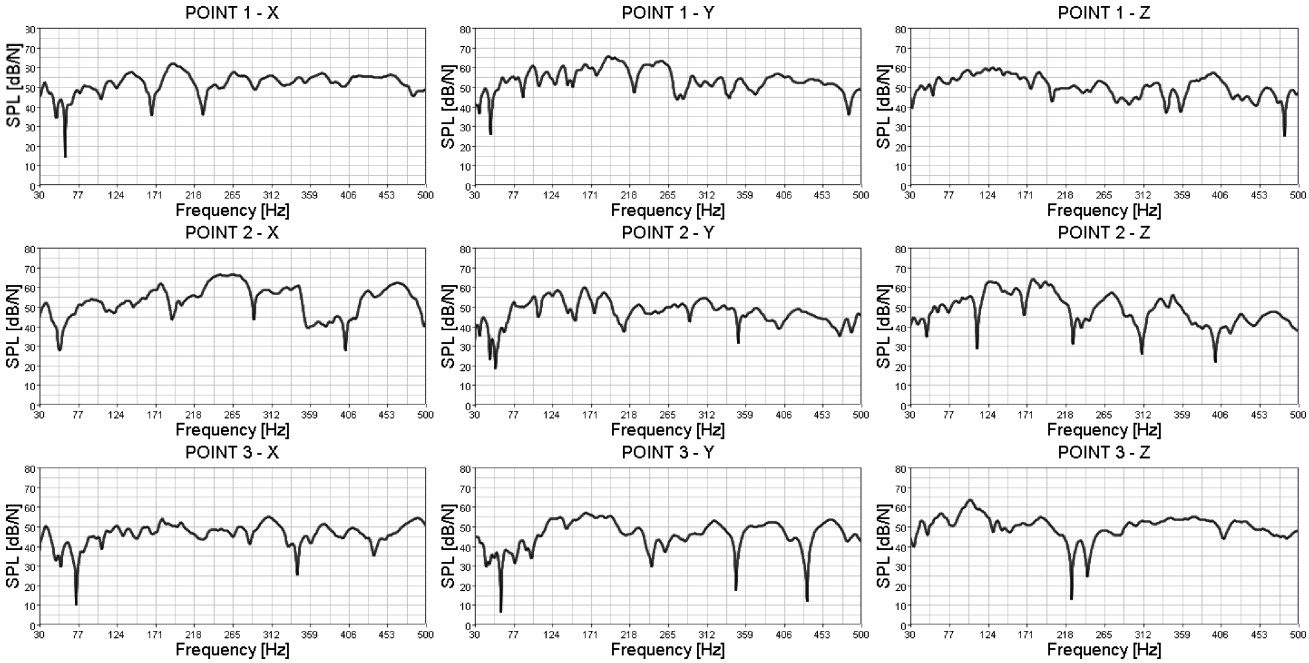

Fig. 12. Popular compact vehicle model; SPL experimental response of the attachment point of the engine (the ordinate grid step is LOG scale).

3. Numerical formulation

This section describes the details of the FEM models of each vehicle. In addition to the modal behaviour of the structure, it is also important to consider the residual vectors to compensate for the higher-order frequencies that are not directly extracted. The mesh size was tuned in 8 elements for each wavelength at 500 Hz and so with an average size of 5 mm.

Table 3 describes the characteristics that make up each virtual model (Komzsik, 2001).

The numerical models were implemented with damping data according to the experimental results to determine how the damping behaviour of these structures would be effected by the frequency response of the various types of vehicles. Additionally, for this numerical study, we used the same categories of vehicles: a pick-up truck and a compact vehicle.

Table 3. Virtual model characteristics.

FE structure – Vehicle 1	FE structure – Vehicle 2
Mass: 352 Kg	Mass: 251 Kg
WELD:5234	WELD:4336
RIGID:622	RIGID:172
RBE3:169	RBE3:0
SPRING:1	SPRING:0
Shell 3 nodes: 15349	Shell 3 nodes: 19122
Shell 4 nodes: 497450	Shell 4 nodes: 593584
Solid 6 nodes: 114	Solid 6 nodes: 120
Solid 8 nodes: 6545	Solid 8 nodes: 7079
Total elements: 536767	Total elements: 633389
Total nodes: 560135	Total nodes: 657227

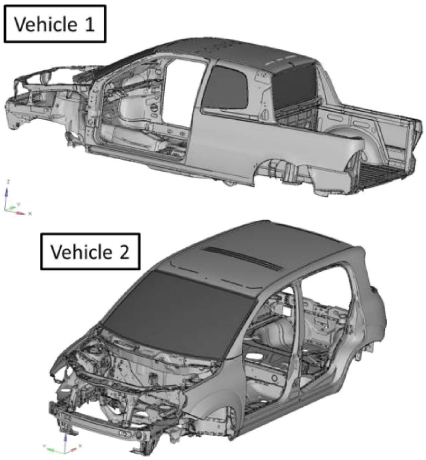

Fig. 13. Numerical models in the body in white version.

For this research, all vehicles were subjected to the same procedure in which HyperMesh 11.0 was used for all computational pre-processing, and NASTRAN software was used for the processing. Figure 13 illustrates the numerical models of vehicles in the body-in-white configuration.

4. Numerical and experimental correlation

The responses of the numerical models were loaded with their respective modal cavity damping (actual variable damping, experimentally extracted from their respective prototype) presented in Fig. 7 and then generated using the SPL acoustic curves. These curves, quantitative comparison of the sound pressure levels (SPL) – Experimental *(continuous line)*, x – Numerical (*dashed line)*, were extracted and compared and are shown in Figs. 14 and 15. All results are on a logarithmic scale.

4.1. Data analysis

Based on the previous results, it is noticeable how the numerical results compare to the experimental results. Next, the challenge that faces NVH engineering simulation is to obtain a standard value of modal cavity damping for the TBIW vehicle model to present the same level of correlation when used with the actual experimentally measured cavity damping values.

Thus, based on the values in Fig. 7, a study was conducted to understand the variation of the average

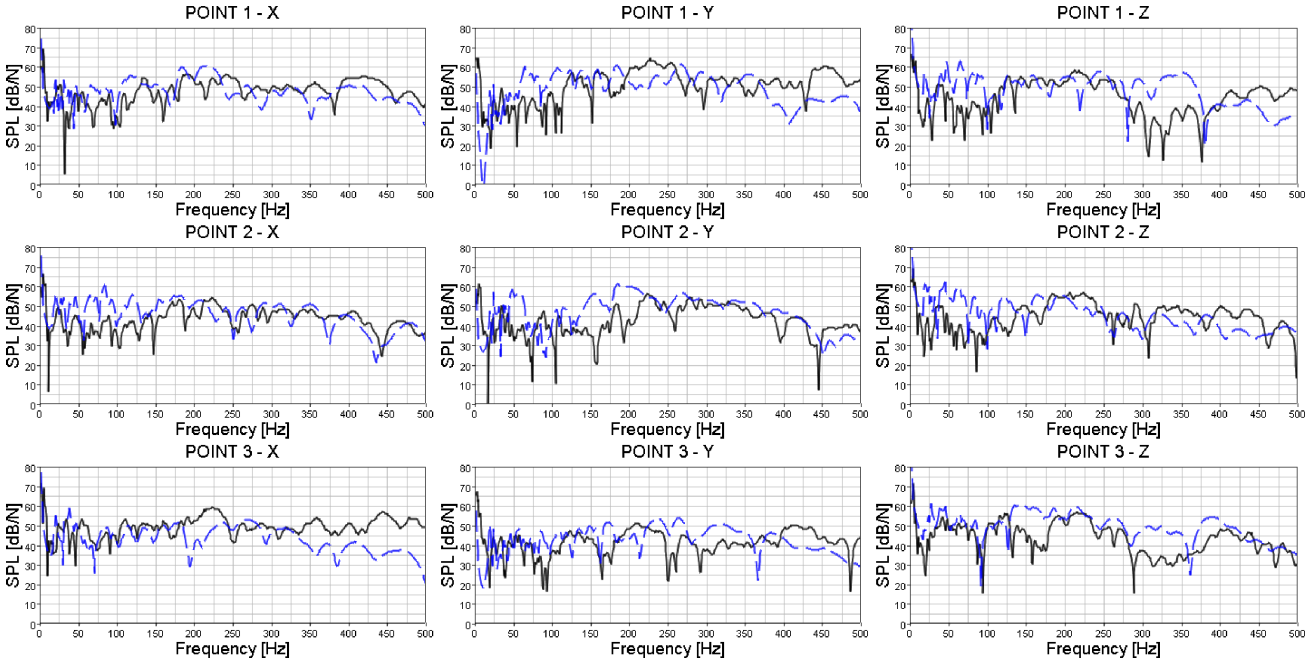

Fig. 14. Pick-up model. Numerical and experimental SPL confrontation of the engine mount (the ordinate grid step is LOG from 0.1).

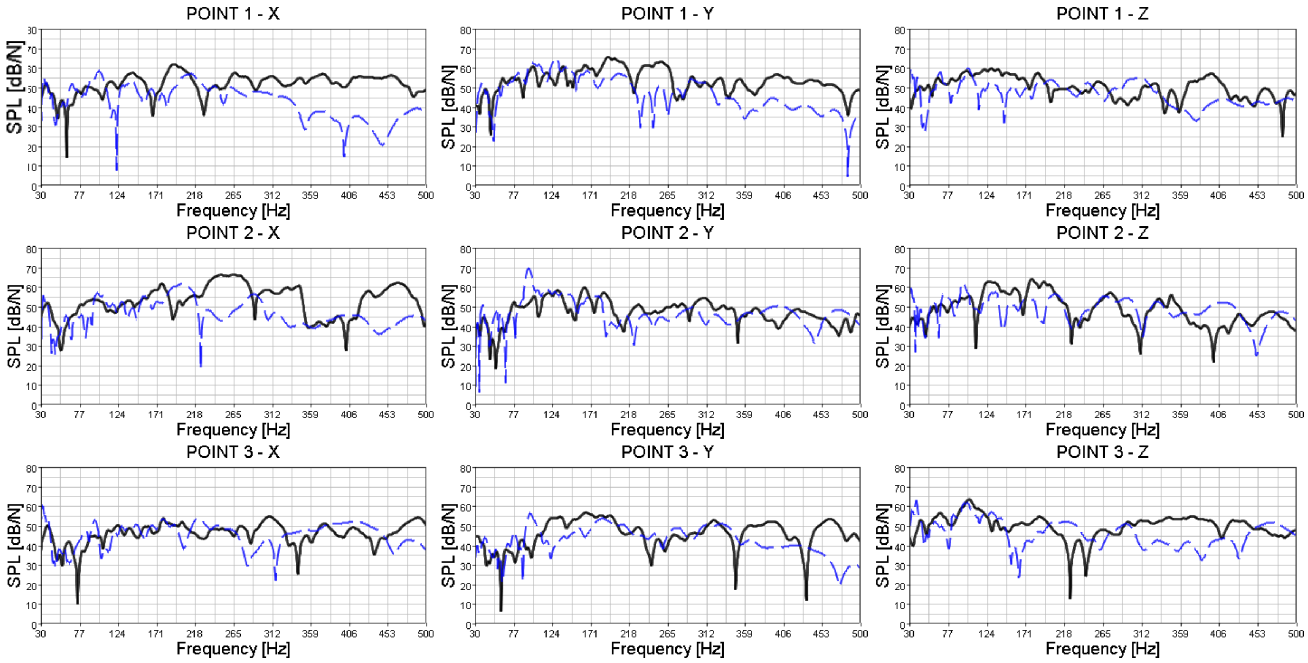

Fig. 15. Popular compact vehicle model. Numerical and experimental SPL confrontation of the engine mount (the ordinate grid step is LOG from 0.1).

damping of these vehicles and the individual difference among them. This result is shown in Fig. 16.

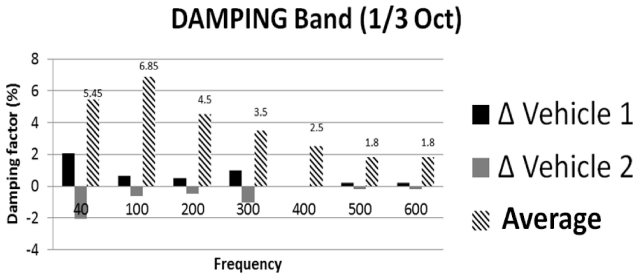

Fig. 16. Overall average of the damping factor for all cavity vehicles and the individual differences.

Observing the behaviour of the average variation of the cavity damping along the frequency, this graph can be separated into two regions: one – up to 100 Hz and the other – up to 600 Hz. For this reason, this study was remodelled by remaking an overall average up to 100 Hz and an average up to 600 Hz. With this methodology, we reached a modal damping that varies in its mean obeying a decreasing damping function.

In this first stage, we have a 6.15% modal cavity damping (100 Hz $< x$), and in the second step, we have a variable function: $\xi(x) = -0.0126(x-100)+6.15$ (to 100 Hz $< x <$ 600 Hz). Figure 17 illustrates this new average and the individual differences of these vehicles at this new average.

With a new average damping (here called damping_design), new results of Sound Pressure Level (SPL)

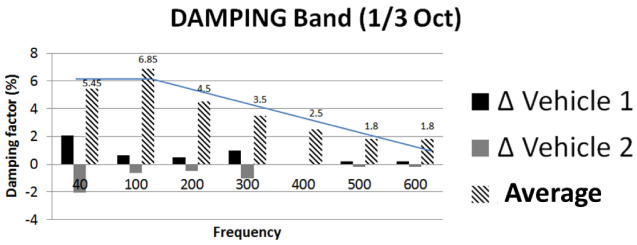

Fig. 17. New general average damping factor (damping_design).

were generated. Figures 18 and 19 compare the numerical results, one with damping measured experimentally and the other generated by this study (damping_design). The curves, **experimental** (continuous black line), numerical **results** with damping experimental values (dashed blue line), and **numerical results** with "damping design" (continuous red line with triangle marks) from the average presented above, were extracted and compared and are shown in these figures. All results are shown on a logarithmic scale.

Analysing the results illustrated in Figs. 18 and 19, the numerical response loaded with their respective modal cavity damping (actual variable damping, experimentally extracted from their respective prototype) and the numerical response using the average of damping (Damping Design) developed in this paper show that the response sound pressure level (SPL) was very close to experimental response (black continuous curve). In this case it is considered "close" when analysing the average of variations of the numerical results and found to be less than 3%.

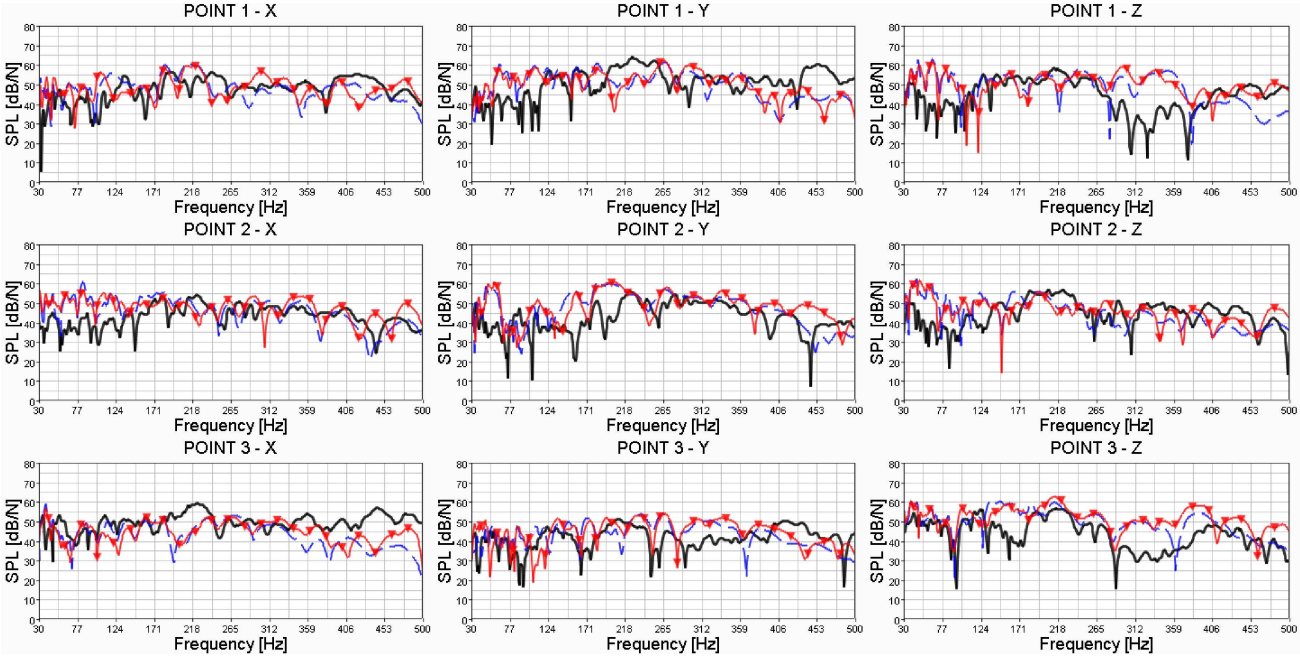

Fig. 18. Pick-up model. Numerical confrontation of SPL models with experimental damping and damping_design of the engine mount point (1,2, and 3) (the ordinate grid step is LOG from 0.1).

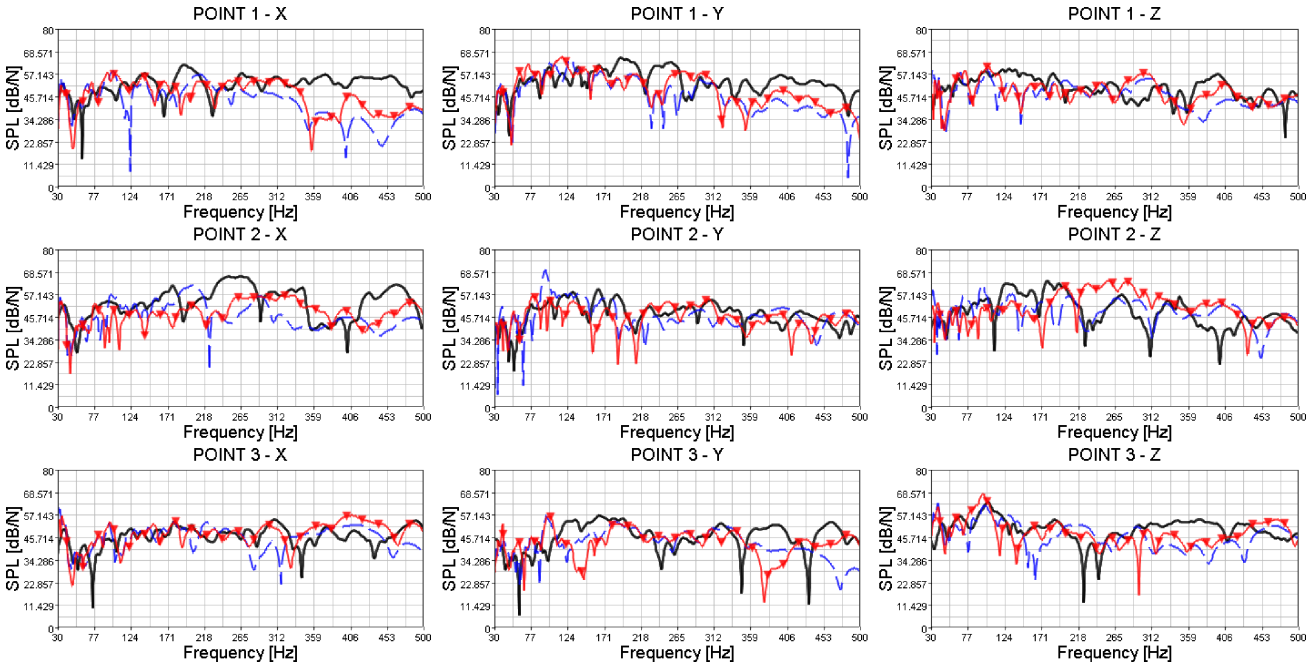

Fig. 19. Popular compact vehicle model. Numerical confrontation of SPL models with experimental damping (constant cavity damping – 6%) and damping_design of the engine mount point (1,2, and 3) (the ordinate grid step is LOG from 0.1).

The average of variations is calculated and compared between the experimental and numerical results using 80 percentile level of the curve. This is the value that includes 80% of samples, with exception of very high values. There are several formulations for calculating this "average". For this research the **Nearest Rank Method** (Johnson, Kuby, 2007) was used.

Using this methodology, the objective is "synthesise a curve in a single value". For calculation on a frequency range (1/3Oct) the following algorithm was used:

The list of N values (between $f_{\min}$ and $f_{\max}$) is **sorted** (ascendant for dynamic stiffness, descendent for SPL). The ordinal rank is calculated according to: the greatest integer that is less than or equal to $P/100 \cdot N$, where P is the complementary to decided percentile ($P = 100 - 80 = 20$) and N is the number of values ($f_{\max} - f_{\min} + 1$).

Example of 80 percentile in 80–200 Hz (80 and 200 included):

$$P = 20, \qquad N = 200 - 80 + 1 = 121,$$
$$n = 20\% \cdot 121 = 24, \qquad n = 24.$$

Position 24 of the sorted list of 121 values is the NVH synthesis.

The methodology described above, Nearest Rank Method, was used to compare the numerical and experimental results that indicated a smaller difference than 3% in the directions X, Y, and Z. This is observed in both vehicles used in this research and at the three points of the engine mount. The points with their respective directions of excitation that do not show good correlation responded best when the damping function was used. An example of this is point 3 in the X direction for the pick-up and point 1 for the X direction. It is also possible to see from the analysis of the results shown in Fig. 18 and 19 that the use of the function $\xi(x) = -0.0126(x - 100) + 6.15$ (to 100 Hz $< x <$ 600 Hz) and 6.15% (to 30 Hz $< x <$ 100 Hz) to represent the modal damping of the cavity of the vehicles used maintained a good numerical-experimental correlation of sound pressure results.

5. Conclusions

Based on the results, there was a good numerical-experimental correlation when using a modal cavity damping function extracted experimentally and including it in the numerical models. Thus, this research sought to ensure the same performance using a standard damping (damping-design) as input as could be used to identify the acoustic behavior of vehicles in the general TBIW configuration.

This study used two types of vehicles as a sample to ensure reliable coverage of the results.

It was observed that the results used for modal damping vary in their mean, obeying a decreasing function such as $\xi(x) = -0.0126(x - 100) + 6.15$ up to 100 Hz and 6.15%. Up to this and when applied to the numerical model, it was observed that the performance in which the variation of the initial result (with damping retrieved from experimental measurements) is very small, in average is less than 0.5 dB. This small variation (0.5 dB) can be found making a difference between the average of the values found in the Figs. 18 and 19 (all points and all directions).

This research that seeks to define a damping function that can be standardised for numerical acoustics problem solving on compact vehicles, presents a first step towards this definition because these values make an appropriate option for the standardisation of values of modal cavity damping on the two categories of vehicles studied, for acoustic analysis, in the early stages of a new automotive project.

Acknowledgment

The authors thank the generous support of the Pontificia Universidade Catolica de Minas Gerais – PUCMINAS; "Coordenação de Aperfeiçoamento de Pessoal de Nível Superior" – CAPES – "National Counsel of Technological and Scientific Development"; Conselho nacional de desenvolvimento cientifico e tecnológico- CNPq – "National Council of Scientific and Technological Development"; Fundação de Amparo à Pesquisa de Minas Gerais – FAPEMIG – "Foundation for Research Support of Minas Gerais"; also to FIAT Automóveis company and IFMG- Federal Institute of Minas Gerais.

References

1. Braess H.H., Seiffert U. (2005), *Handbook of Automotive Engineering*, 1st ed., Ed. Hans-Hermann Braess, USA, Pennsylvania, pp. 67–69.
2. Cameron C.J., Wennhage P., Göransson P. (2010), *Prediction of NVH behaviour of trimmed body components in the frequency*, Appl. Acoust., **71**, 8, 708–721, DOI: 10.1016/j.apacoust.2010.03.002.
3. Davy J.L., Phillips T.J., Pearse J.R. (2014), *The damping of gypsum plaster board wooden stud cavity walls,* Appl. Acoust., **88**, 52–56.
4. Ferreira T.S., Moura F., Magalhões P. (2013), *Sensitivity analysis of numerical and experimental comparison by nvh finite element simulation in "trimmed body" to different excitation points of a vehicle in the frequency range until 500 Hz*, 22nd International Congress of Mechanical Engineering (COBEM), ISSN 2176-5480, 22, 1842–1849.
5. Hörnlund M., Papazoglu A. (2005), *Analysis and measurements of vehicle door structural dynamic response*, Master's Dissertation, Lund University, Sweden.
6. Johnson R., Kuby P. (2007), *Applied Example 2.15. The 85th Percentile Speed Limit: Going with 85% of the Flow*, [in:] Elementary Statistics (10th ed.), Cengage Learning, p. 102, ISBN 9781111802493.
7. Komzsik L. (2001), MSC. NASTRAN., Numerical User's Guide, The MacNeal-Schwendler Corporation, Los Angeles, CA, USA.
8. Kumar G., Walsh S.J., Krylov V.V. (2013), *Structural – acoustic behaviour of automotive-type panels with dome-shaped indentations*, Applied Acoustics, **74**, 6, 897–908.
9. Kurosawa Y., Yamaguchi T. (2013), *Finite Element Analysis for Damped Vibration Properties of Panels Laminated Porous Media*, World Academy of Science, Engineering and Technology, Japan, **7**, 2013-06-20, 78.
10. Lim T.C. (2000), *Automotive panel noise contribution modeling based on finite element and measured structural-acoustic spectra*, Appl. Acoust, **60**, 505–519.
11. LMS International (2013), LMS PolyMAX, *A Revolution in Modal Parameter Estimation,* Leuven, Belgium.

12. Moura F., Ferreira T.S., Danti M., Meneguzzo M. (2012), *Numerical and experimental comparison by NVH Finite Element Simulation in "Body in White" of a vehicle in the frequency range until 800 Hz*, SAE Technical Paper, 2012-36-0629, DOI: 10.4271/2012-36-0629.

13. Peeters B., Van der Auweraer H., Guillaume P., Leuridan J. (2004), *The PolyMAX frequency-domain method: a new standard for modal parameter estimation*, Shock and Vibration, **11**, 3–4, 396–409.

14. Performance Standard (2004), *Vehicle and Shell – Acoustic/vibration transfer functions analysis*, Fiat Auto, N.7 – R0151.

15. Pockszevnicki C., Rodrigues E., Ferreira T.S., Barbosa R., Vieira A., Silveira M. (2011), *Finite element analysis considering material porosity*, SAE Technical Paper 2011-36-0136, DOI: 10.4271/2011-36-0136.

16. Rao, Singiresu (2008), *Vibrações Mecânicas*, 1st ed., Ed: Pearson, Brasil, São Paulo, pp. 82–85.

17. Zhang W., Vlahopoulos N., Wu K. (2005), *An energy finite element formulation for high-frequency vibration analysis of externally fluid-loaded cylindrical shells with periodic circumferential stiffeners subjected to axisymmetric excitation*, Journal of Sound and Vibration, **282**, 3–5, 679–700, DOI: 10.1016/j.jsv.2004.03.063.